Global Journal of Researches in Engineering: A
Mechanical and Mechanics Engineering
Volume 14 Issue 6 Version 1.0 Year 2014
Type: Double Blind Peer Reviewed International Research Journal
Publisher: Global Journals Inc. (USA)
Online ISSN: 2249-4596 & Print ISSN: 0975-5861

Constant Pitch Propeller Design for Low Subsonic Airplane

By Arif Ahmed Sohel, Md. Abdus Shamir Talukder
& Dr. Mohammad Arif Hasan Mamun
Bangladesh University of Engineering and Technology, Bangladesh

Abstract- Constant pitch propeller whose blade angle is fixed with respect to hub is suitable for low speed airplane. The objectives of this thesis are to determine thrust, torque and the performance of the low subsonic airplane propeller. The thesis has been carried out by the two different approaches- Analytical and Computational Fluid Dynamic (CFD) simulation. The Analytical Method using "Propeller Blade Element Theory" is one of the most effective methodologies available for determining the thrust and torque produced by the propeller. On the other hand, the Computational Fluid Dynamic simulation has been used to simulate and capture the performance of the propeller. Through both methodologies, the propeller performance was analyzed and compared. The results obtained were tabulated and the corresponding graphs were plotted. Both methods suggest that the thrust and torque change with the change in relative velocity. Besides, there are several factors that contribute to the variations in results of the Analytical method and CFD Simulation.

Keywords: CFD, constant pitch, blade element theory, advance ratio, airfoil, coefficients of thrust, torque, power, etc.

GJRE-A Classification : FOR Code: 091399p

Strictly as per the compliance and regulations of:

Constant Pitch Propeller Design for Low Subsonic Airplane

Arif Ahmed Sohel [α], Md. Abdus Shamir Talukder [σ] & Dr. Mohammad Arif Hasan Mamun [ρ]

Abstract- **Constant pitch propeller whose blade angle is fixed with respect to hub is suitable for low speed airplane. The objectives of this thesis are to determine thrust, torque and the performance of the low subsonic airplane propeller. The thesis has been carried out by the two different approaches- Analytical and Computational Fluid Dynamic (CFD) simulation. The Analytical Method using "Propeller Blade Element Theory" is one of the most effective methodologies available for determining the thrust and torque produced by the propeller. On the other hand, the Computational Fluid Dynamic simulation has been used to simulate and capture the performance of the propeller. Through both methodologies, the propeller performance was analyzed and compared. The results obtained were tabulated and the corresponding graphs were plotted. Both methods suggest that the thrust and torque change with the change in relative velocity. Besides, there are several factors that contribute to the variations in results of the Analytical method and CFD Simulation.**

Keywords: CFD, constant pitch, blade element theory, advance ratio, airfoil, coefficients of thrust, torque, power, etc.

I. Introduction

An aircraft propeller is one of the most common important parts in the aircraft. It is an airfoil section designed to generate the aerodynamic forces. The propeller provides the necessary force i.e. thrust to push the aircraft through the air. Thrust is the component of the aerodynamic force that is parallel to the axis of rotation of the propeller. A propeller achieves a specified level of thrust by giving a relatively small acceleration to a relatively large mass of air. Maximizing thrust while minimizing the torque necessary to turn a propeller has becomes one of the most important aspects of good propeller design. The power that must be supplied by the engine is the multiplication of the torque required to turn the propeller and the angular velocity. The thrust developed by the propeller multiplied by the airspeed of the aircraft is called the propulsive power. The aircraft is propelled forward against the airframe drag by this power. The ratio of the propulsive power to the brake power for a propeller gives the propulsive efficiency which is one of the important measures of propeller performance. The thrust developed by the propeller when the aircraft is stationery is called the static thrust. This thrust is important for a propeller to produces high static thrust in order to accelerate the aircraft during takeoff.

In order to design an aircraft propeller, Computational Fluid Dynamic (CFD) analysis has been done to simulate the fluid flow over a body to solve and analyze the aerodynamic properties of a body. Moreover, analytical approach has been used to compare the result gathered from the CFD simulation.

In the time of rapid industrial development along with the current competition in the market has required companies to improve products and create more innovation compared to other products. Aviation industry is also on that trend, and the propeller performance plays an important role. A good propeller should meet the requirements of the flight and push the aircraft with high performance on the aerodynamic characteristics.

For studying these characteristics of the propeller, the numerical study seems to be the best way to accomplish that goal. In particular, the application of CFD simulation software to calculate the propeller aerodynamics is not so new study now and it has become popular methods. Today it becomes most powerful compared to other methods as well as experience or the other traditional methods. The present works focus on numerical simulation of the propeller at different rotating speed. Specific studies were conducted with the flight speed change, a fixed number J from 0 to 1. From these results such as pressure field, we can evaluate the performance of the propeller in the range of the flight velocity.

By using the mathematical models with considered assumptions, simulation results allow the predictions on propeller performance. The simulation has helped save time, effort and cost a lot for the design and manufacture of propellers.

II. Physical Model

Propeller blade has different airfoil shape; the shape varies quite a lot from root to tip. In practice a large number of different airfoils are used to make up one propeller blade but we designed our propeller simply taking only one airfoil along the blades. There are hundreds of airfoils suitable for this application but we think it is better to make a choice of an airfoil containing flat bottom surface. We are going to select NACA 4412 (Fig. 1) flat bottom airfoil used in a lot of propeller

Author: Department of Mechanical Engineering, Bangladesh University of Engineering and Technology, Dhaka-1000.
e-mails: arifahmed07.buet.me@gmail.com, shamir.buet@gmail.com, arifhasan@me.buet.ac.bd

designs in the past, and is also used today for simple designs.

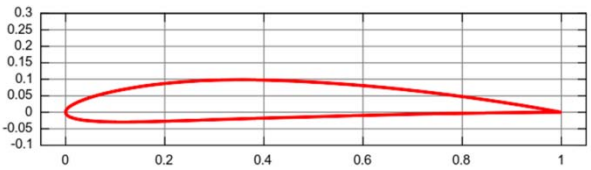

Figure 1 : NACA4412 airfoil [14]

In this design one blade has been considered which consists of 10 sections each having different airfoil shape, and representing different chord length & thickness.

The front plane has been taken as the reference plane in the Solid works part file and 10 more planes were created which are equally spaced. Plane 1 was at 2.4 inch far from reference plane and other 9 more planes were placed successively maintaining 2.4 inch distance between two consecutive planes up to 24 inch. The 2.4 inch difference between reference and 1st plane was kept for propeller hub. Airfoil data points from text file are imported to draw profile curves on each of the 10 planes by "curve through XYZ points" commands. These curves are converted into sketches for every slice of the blade sections. Fig. 2 represents a sample array of slices inserted into a Solid Works part file.

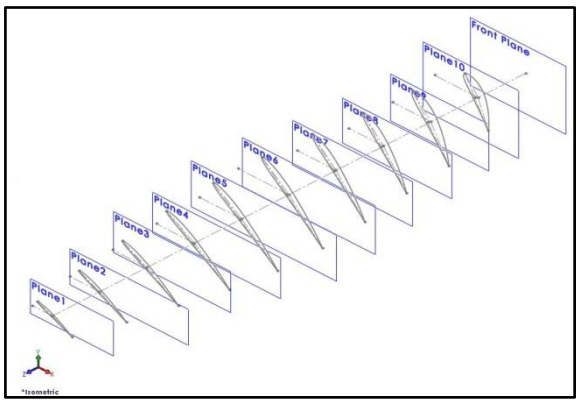

Figure 2 : array of propeller cross sections

The airfoil sections are placed on a line such a way that the line goes through the center of gravity of each section. Because, unbalanced exists when the center of mass does not coincide with the center of rotation, when the mass center axis is different to its running center axis. The centrifugal force due to the unbalance causes the device to vibrate. This vibration causes wear to the bearings, creates unnecessary noise, and can result in complete failure. "Mass properties" command of the "Evaluate" tab was used to determine these gravity centers of the sections. This will keep the propeller vibration free during rotation due to the balanced blade mass distribution.

Then the section profiles are rotated in the design geometric angles of the respective sections that will ensure the design pitch for the rotating propeller. "Loft" feature was used to create a solid body by lofting from root to tip of the section's profile sketches. Automatic linear twist distribution is generated in the blade according to the geometric angles given in the profiles. Tip of the blade is rounded by using dome features.

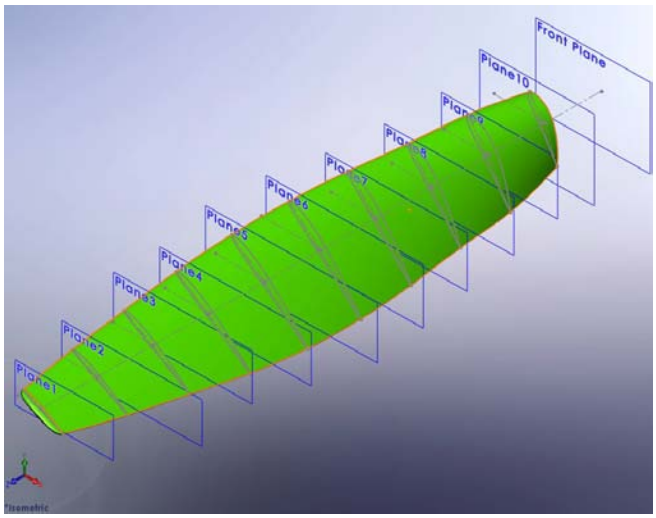

Figure 3 : propeller blade with sliced sections

Propeller hub is inserted in the origin of the part drawing which looks like a cylinder, and this is done by using the "boss extrude" command on a circular profile of 5.1inch diameter. After an array operation of the blade about the origin, blades are added with the hub. "Fillet" feature is used in the joints between the hub and blades. A pointy dome is created on the hub to reduce the drag.

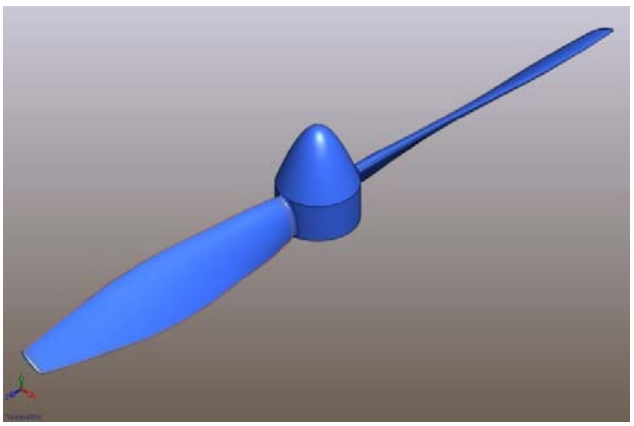

Figure 4 : Final propeller design

III. Mathematical Model

Development of a rational propeller theory begins with the work of Rankine and Froude with their interest in moving propulsion, but the fundamental principle is the same for water and air. They developed the fundamental momentum relation governing a propulsive device in fluid medium.

Stefan Drzewiecki however, was the first to rigorously examine and apply Blade Element Theory (BET). He performed his work between 1892 and 1920. BET is very similar to the Strip Theory for fixed wing aerodynamics. The blade is assumed to be composed of numerous, miniscule strips that are connected from tip to tip. The lift and drag are estimated at the strip using the 2-D airfoil characteristics of the section.

Also, the local flow characteristics are accounted for in terms of climb speed, inflow velocity, and angular velocity. The section lift and drag may be calculated and integrated over the blade span. BET is a very useful tool for the engineer. He or she may perform a fairly detailed local analysis of the rotor in a short amount of time.

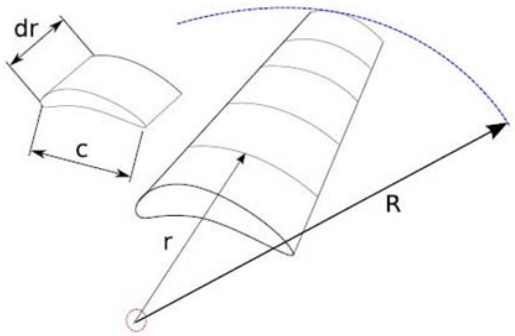

Figure 5 : Schematic of propeller blade

A propeller blade is simply a twisting wing (Fig. 5) which produces lift and drag. The two most important performance parameters for the design and analysis of a propeller are the thrust and torque.

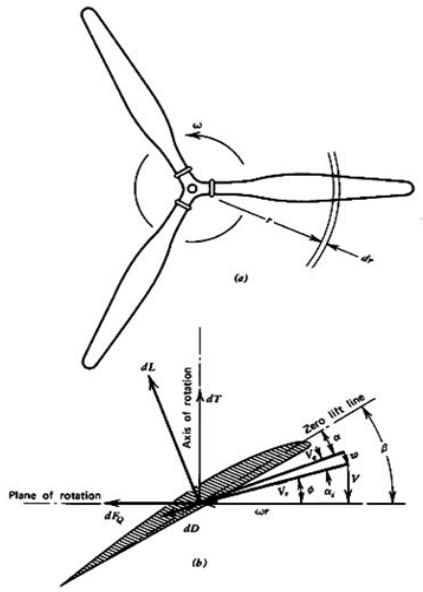

Figure 6 : Schematic of propeller cross-section

Fig. 6 shows a cross section of the blade. The force exerted on the span wise extension of the blade element is the resultant of two components i.e. lift and drag.

Where,

v=Incoming air velocity

ωr =tangential velocity of the rotating propeller

We can write the expressions of the elemental thrust and torque for the radial element (dr) on one of the blades:

$$dT = dL\,Cos\,\varphi - dD\,Sin\,\varphi$$
$$= \tfrac{1}{2}\,\rho\,VR^2 c\,dr\,(C_l Cos\,\varphi - C_d Sin\,\varphi)$$
$$dQ = (dL\,Sin\,\varphi + dD\,Cos\,\varphi)r$$
$$= \tfrac{1}{2}\,\rho VR^2 c\,dr\,(C_l Sin\,\varphi + C_d\,Cos\,\varphi)\,r$$

If

Resultant velocity, $V_R = V_\infty / Sin\,\varphi$

& Dynamic pressure, $q = \tfrac{1}{2}\rho\,V_\infty^2$,

Then the elemental thrust,

$$dT = q\,c\,dr\,(C_l Cos\,\varphi - C_d\,Sin\,\varphi)/\,Sin^2\,\varphi$$

The elemental torque,

$$dQ = q\,c\,r\,dr\,(C_l Sin\,\varphi + C_d\,Cos\,\varphi)/\,Sin^2\,\varphi$$

Where,

dL= elemental lift

dD= elemental drag

Cl = coefficient of lift

Cd= coefficient of drag

ρ = density of air

C = chord length

Φ= angle subtended by relative velocity

V_∞=incoming air velocity

Propeller thrust and torque are computed by integrating the equations of the elemental thrust and torque from root to tip of the blade. For number of blades B,

The total thrust,

$$T = qB\int_0^R c\,dr\,(C_l Cos\,\varphi - C_d\,Sin\,\varphi)/\,Sin^2\varphi$$

Simplified

$$T = q\,B\,R\int_0^1 c\,dr\,(C_l\,Cos\,\varphi - C_d Sin\,\varphi)/\,Sin^2\,\varphi; \qquad (1)$$

Where x=r/R

The total torque

$$Q = q\,B\int c\,r\,dr\,(C_l\,Sin\,\varphi + C_d\,Cos\,\varphi)/\,Sin^2\,\varphi$$

Simplified

$$Q = q\,B\,R^2 \int_0^1 c(r/R)dr\,(C_l \mathrm{Sin}\,\varphi + C_d\,\mathrm{Cos}\,\varphi)\,\mathrm{Sin}^2\,\varphi \;;(2)\text{where } x=r/R)$$

Elemental blade efficiency, [1] [2] [3]

$$\eta = \frac{C_l\,\mathrm{Cos}\,\varphi - C_d\,\mathrm{Sin}\,\varphi}{C_l\,\mathrm{Sin}\,\varphi + C_d\,\mathrm{Cos}\,\varphi}\tan\varphi$$

The first important task is the selection of an airfoil to design a propeller. The selected airfoil must maintain the aerodynamic characteristics that will provide lift and drag required for the thrust (propulsive force for airplane) and torque (available torque from engine shaft to rotate propeller).

As the maximum operating altitude ranges up to 25,000 feet and for smaller aircraft with propellers and normally aspirated engines, the service ceiling (maximum altitude where 100 feet per minute climb can be maintained) ranges 12,000-14,000 feet, we choose 10,000 feet as the design altitude for the airplane that can be propelled by our propeller.

Followings are the design characteristics:

Altitude- 10,000 feet (3048 m)

Airplane speed- 50ms-1

Airfoil- NACA 4412

Diameter- 48 inch (1.22 m)

Pitch- 75 inch (1.905 m)

Operating pressure [5],

P= 101325 e^ (-[(M×g×h) ÷(R×T)])

Air density, ρ=P/RT=0.854 kgm-3 where T=288 k

Sound velocity, C= (KRT)-1/2=340ms-1 where k=1.4

IV. Numerical Procedure

a) Computational Design

The computational design is comprised of a frame of 2.5m×9.5m×2.5m. Now the boundary conditions are assigned as; 'Surface A' is the 'Velocity Inlet' of 50m/s uniform velocity, 'Surface B' is the 'Pressure Opening' of 70600pa'Surface C, D, E&F' are considered as the 'Ideal Wall'

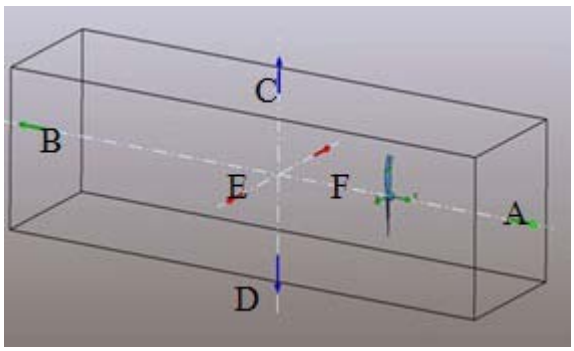

Figure 7 : Computational domain

An enclosed volume is considered as rotating region of the propeller. Here propeller is kept constant and rotating frame indicating the rotating region rotates about the propeller axis at same RPM of the propeller but opposite in direction.

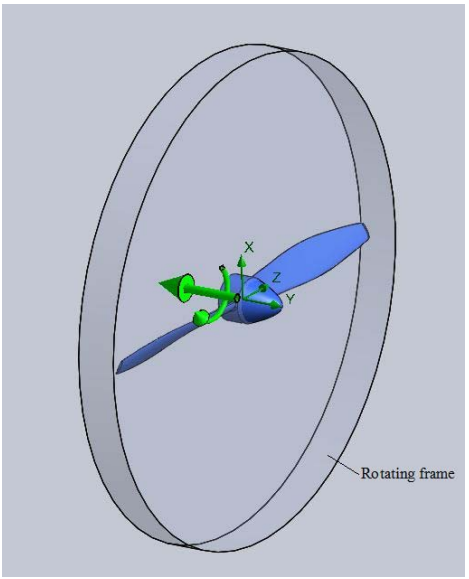

Figure 8 : Computational domain with rotating frame

b) Computational Meshing

In computational domain of flow simulation computational mesh is rectangular everywhere, so the mesh cells' sides are orthogonal to the specified axes of the Cartesian coordinate system and are not fitted to the solid/fluid interface. As a result, the near-walls of mesh cell are cut by the solid/fluid interface. Nevertheless, due to special measures, the mass is treated properly in these cells named partial.

At first a basic mesh is constructed. For that, the computational domain is divided into slices by the basic mesh planes, which are evidently orthogonal to the axes of the Cartesian coordinate system. The basic mesh is determined only by the computational domain and does not depend on the solid/fluid interfaces.

Then, the basic mesh cells intersecting with the solid/fluid interface are split uniformly into smaller cells in order to capture the solid/fluid interface with mesh cells of the specified size (with respect to the basic mesh cells). The following procedure is employed each of the basic mesh cells intersecting with the solid/fluid interface is split uniformly into 8 child cells; each of the child cells intersecting with the interface is in turn split into 8cells of next level, and so on, until the specified cell size is attained.

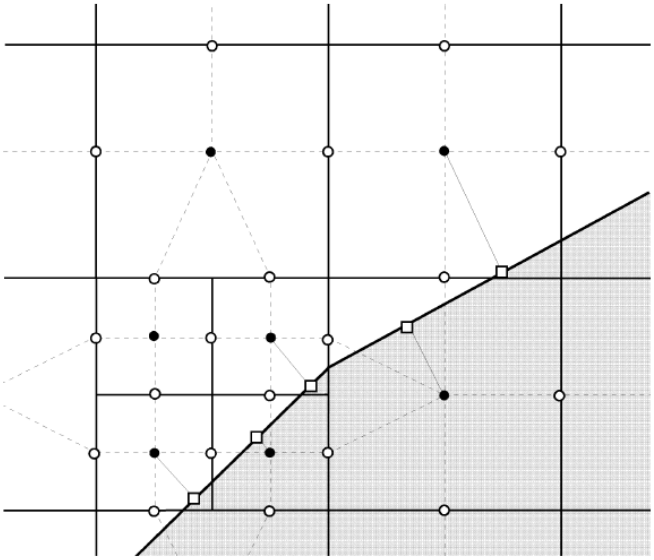

Figure 9 : Computational mesh cells at the solid/fluid interface

At the next stage of meshing, the mesh obtained at the solid/fluid interface with the previous procedure is refined in accordance with the solid/fluid interface curvature.

Finally, the mesh obtained with these procedures is refined in the computational domain to satisfy the so-called narrow channel criterion: for each cell lying at the solid/fluid interface, the number of the mesh cells (including the partial cells) lying in the fluid region along the line normal to the solid/fluid interface and starting from the center of this cell must not be less than the criterion value. Otherwise each of the mesh cells on this line is split into 8 child cells. As a result of all these meshing procedures, a locally refined rectangular computational mesh is obtained and used then for solving the governing equations on it.

After completion of mesh generation, flow Simulation solves the Navier-Stokes equations (formulations of mass, momentum and energy conservation laws for fluid flows) with the finite volume (FV) method on a spatially rectangular computational mesh designed in the Cartesian coordinate system.

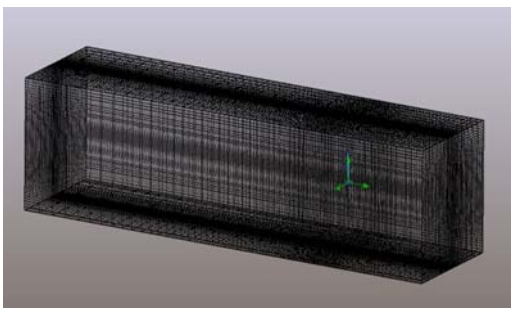

Figure 10 : Basic mesh

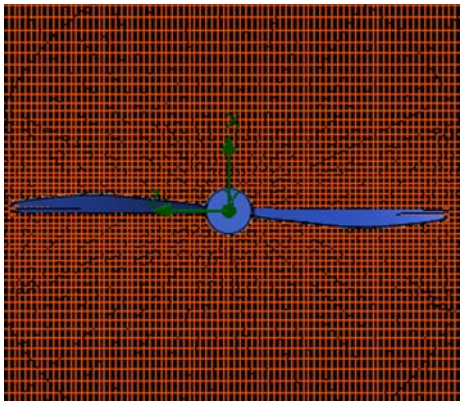

Figure 11 : Basic mesh (Top view)

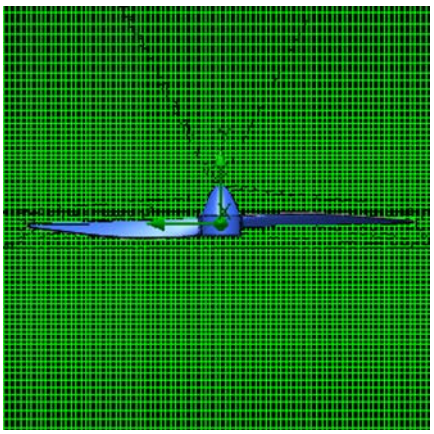

Figure 12 : Basic mesh (Right side View)

V. Results and Discussion

a) Analytical Result

To calculate elemental thrust and torque from eqn. (1) & (2) we have calculated **φ**, C_l, C_d & Chord length which varies with respect to the radial distance from the propeller center for 10 sliced sections. The tangential velocity changes with distance from the root to tip that contribute in the change of the relative velocity while the incoming air velocity remains fixed. This variation in the relative velocity changes the angle of attack in order to keep the pitch of the propeller fixed. We have calculated Cl and Cd for different angle of attack by using the Characteristics of NACA 4412 chart shown in the Fig. 13.

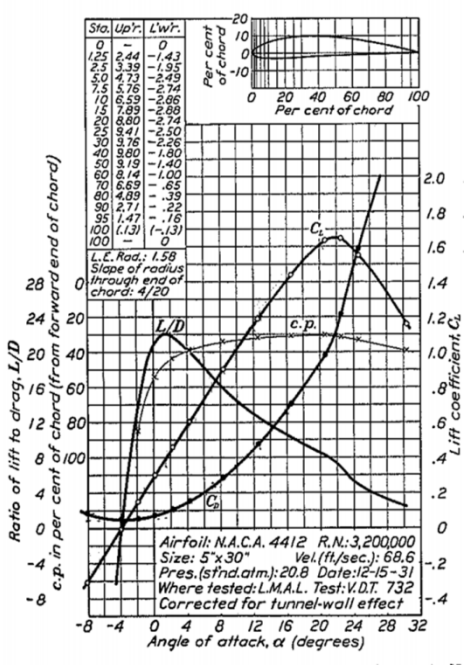

Figure 13 : Characteristics of NACA 4412

Dynamic pressure $q_\infty = \frac{1}{2} \rho V_\infty^2 = 1067.68$ Pa
The angle subtended by relative velocity VR [7], $\varphi = \beta$ (blade pitch angle)-α (Angle of attack)

We have plotted dCT/dx vs X &dCQ/dx vs X in the Fig. 14 to get the equations for dT/dx and dQ/dx. Therefore,

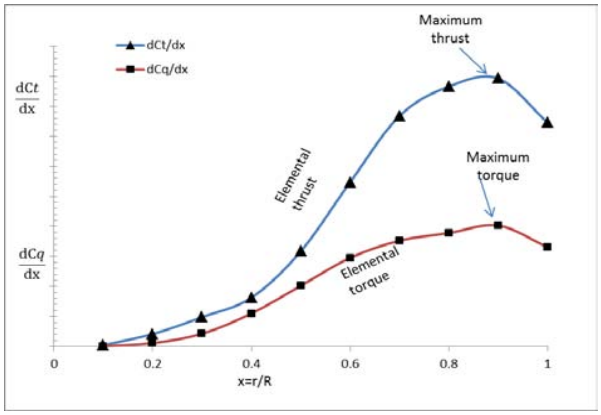

Figure 14 : Elemental coefficients gradient vs radial distance from root of the propeller

Here,

Total thrust, T= ∫ (dT/dx) dx

$$= \int_{0.1}^{1} (39748x^6 - 96725x^5 + 58676x^4 + 11010x^3 - 15011x^2 + 4063.1x - 266.78)dx = 817.24\ N$$

Total torque, Q= ∫ (dQ/dx) dx

$$= \int_{0.1}^{1} (-78162x^6 + 259394x^5 - 334610x^4 + 206529x^3 - 60258x^2 + 8159.6x\ 388.43)dx = 395.54\ Nm$$

By analyzing the curve of the gradient of the elemental thrust and torque coefficient plotted against span wise direction of a blade (root to tip distance), it is observed that maximum thrust and maximum torque cannot be obtained for the same element. For the maximum thrust, the torque obtained is somewhat less than the maximum torque and the thrust obtained is less than its maximum value when the torque is maximum. The maximum thrust and the maximum torque typically occur at the outer half of the propeller blade and the lower half contributes little to the thrust and torque. So, one need to be much careful while designing the propeller that the thrust needs to be distributed in a manner so that together the blended propeller would give the necessary thrust which is required for flying the aircraft.

b) CFD Result

Flow simulation of CFD software provides total thrust and torque 1007 N and 311.19 Nm respectively.

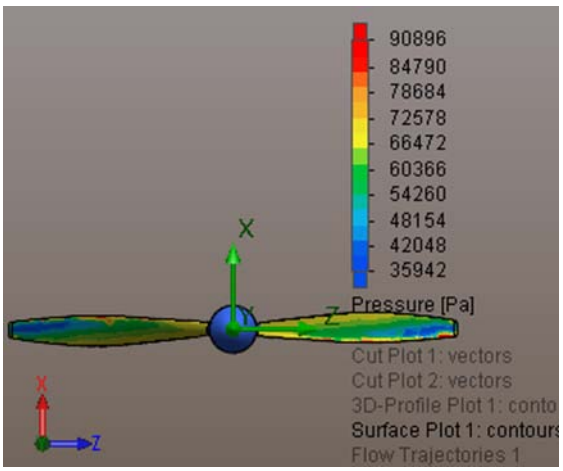

Figure 15 : Suction side pressure distribution (Upstream)

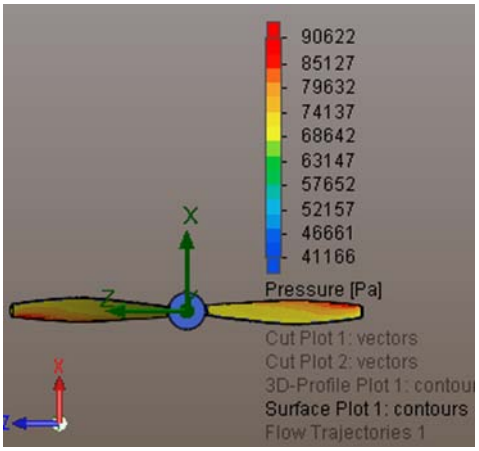

Figure 16 : Pressure side pressure distribution (Downstream)

Pressure distributions on the blade surface are plotted in Fig. 15 for suction side and Fig. 16 for pressure side. As seen, the pressure distributions show a typical pattern that a very high pressure gradient occurs at the leading and trialing edges.

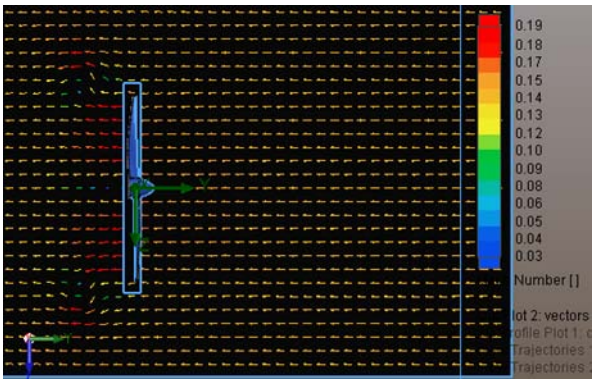

Figure 17 : Velocity vector plot

Velocity vector plot in longitudinal plane is drawn in Fig. 17. As shown, due to the action of propeller, fluid is sucked to the propeller disk and starts to accelerate in front of the propeller toward downstream direction and there is swirling motion due to centrifugal action of the flow in the downstream.

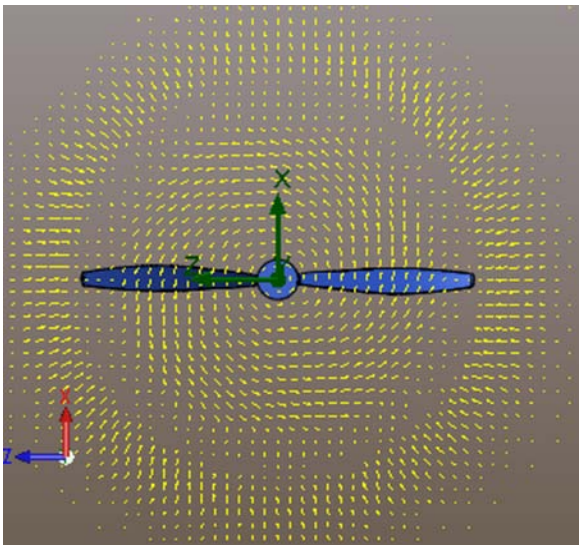

Figure 18: Cross flow vector behind propeller

Cross flows at propeller downstream are given in Fig. 15; a strong swirling flow can be seen. Finally, Fig. 19 shows velocity vector of the propeller blade on the top plane. It is seen that Mach no. is highest on the leading edge of the blade due to suction action of the propeller.

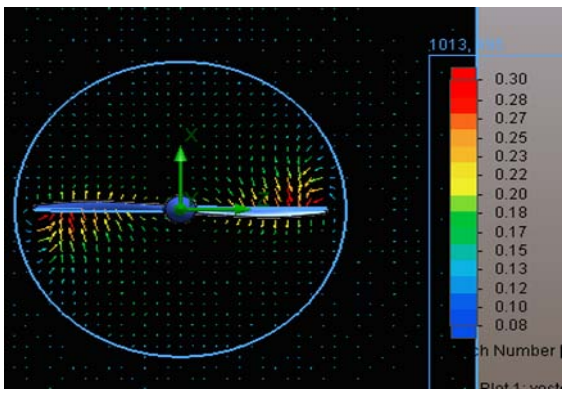

Figure 19 : Velocity vector presenting Mach no

To have a general view of the flow pattern, the velocity vector plots are given in Fig. 20, 21, 22 for various distances from the root.

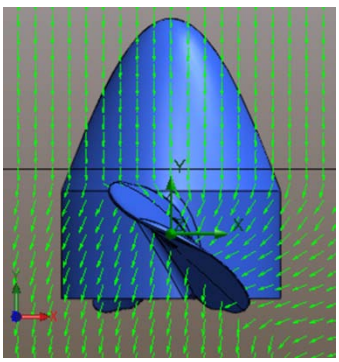

Figure 20 : Velocity vector at .5R section

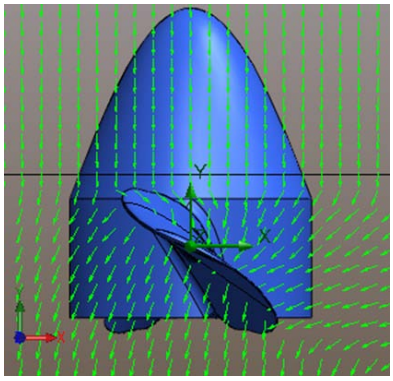

Figure 21 : Velocity vector at .7R section

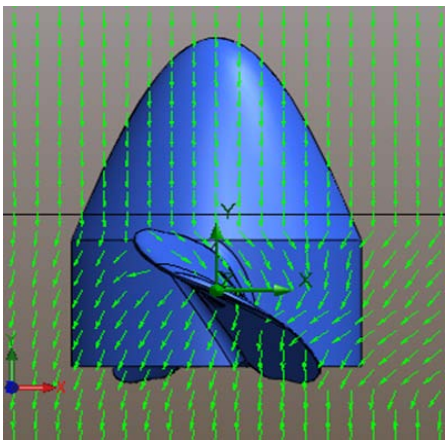

Figure 22 : Velocity vector at .9R section

The propeller sucks the flow in the opposite direction of the free stream flow and the free stream flow becomes slow down in front of the propeller. However, as seen in Figures.

Highest design RPM for our propeller is 4525 which limits Mach number to .85 at the tip of our propeller. So, it is in the transonic range 0.8-1.2, but it is desirable to drop the Mach no. to subsonic range when RPM decrease because of inconsistency of the supplied power to the propeller. In propeller design prospect, Mach no is tried to keep below .85 to avoid the shockwave due to the sonic flow around the propeller.

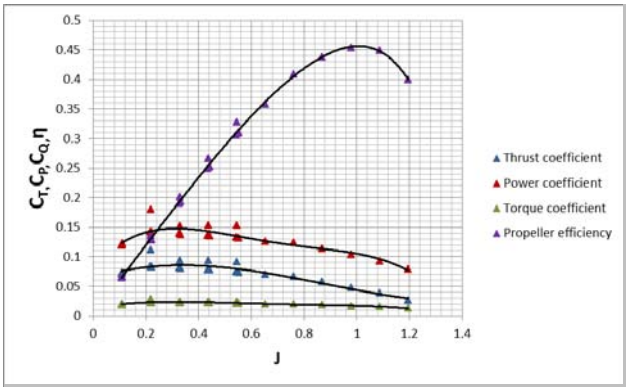

Figure 23 : Propeller coefficients vs advance ratio

From graph it is evident that highest thrust and power coefficient occur at lower advance ratio and efficiency is highest at higher advance ratio. For fixed blade propeller the pitch is fixed, angle of attack will decrease as the forward velocity of aircraft increases. Although this will result in an efficiency increase initially, further increasing the velocity will make the angle of attack zero and the Propeller will not be able to generate thrust which is avoidable by using variable pitch propeller. In the figure cruise point will be somewhere nears the point of highest efficiency, for which we will lose some thrust and power, but there still enough thrust and torque to propel the aircraft.

The performance graph of our propeller that we have obtained is similar to the characteristics graph of the propeller which is represented in Fig. 24.

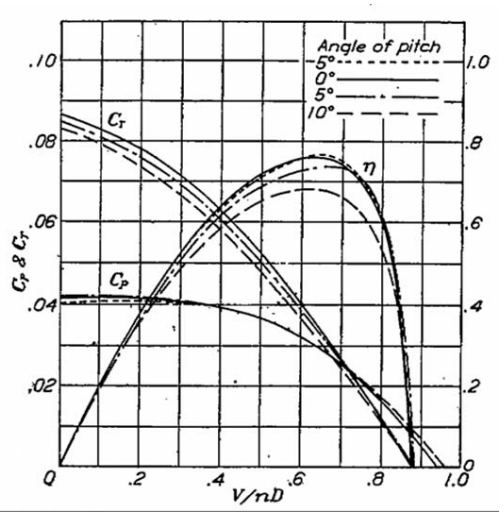

Figure 24 : Characteristics graph of propeller no. 4412

VI. Conclusion

From CFD analysis the thrust and torque for our propeller are 1007N and 311.19Nm which are 22.3% and 21.3% less than the theoretical calculated values. At 4525 RPM the propeller will provide maximum efficiency if the aircraft speed is 92ms-1 and there are 47% and 33.33% reduction in thrust and torque respectively than the maximum value that can be obtained by this propeller.

References Références Referencias

1. Anderson, J. D. Jr. (2010*) Fundamental of Aerodynamics* [SI Units]. Fifth edition. New Delhi: Tata McGraw Hill.
2. Fox, R. W. McDonald, A. T. and Pritchard, P. J. (2009) *Introduction to Fluid Mechanics*. Fifth Edition. Singapore: John Wiley and Sons Inc.
3. Theoretical background material influenced Strongly by Unified Engineering Lecture notes, MIT. Section 11.7.

4. Von Mises, Blade Element Theory, Theory of Flight By Richard. Prof. Bhakskar Roy, Video lectures on propeller, Dept. of Aerospace Engineering, IIT, Bombay.
5. Federal Aviation Regulations, Amendment 23, FAR 23.1527.
6. U.S. Standard Atmosphere, 1976, U.S. Government Printing Office, Washington.
7. Melbourne, Australia, Dynamic Balancing, Industrial Standards, International Standards.
8. Magdalena R. V. Sta. Maria and Mark Z. Jacobson, Examining the Effects of Wind Farms on Array Efficiency and Regional Meteorology, Stanford University -Presented at Wind power 2007.
9. McCormick, B.W., Aerodynamics Aeronautics and Flight Mechanics, Wiley, New York, 1979.
10. Shethal Thomas Kodiyattu, Design of a propeller for downwind faster than the wind vehicle, San Jose State University, (2010).
11. NACA report no. 460,306.
12. Article on Compressibility: Selection of propeller airfoil section (Prandtl-Glauert rule) by Joe Supercool.
13. Monal Pankaj Merchant, Propeller performance measurement for low Reynolds number unmanned aerial vehicle applications, B. S., Wichita State University, (2004).
14. NACA report no.389.
15. Flow Simulation 2012 Technical Reference 1-49 of simulation software package.

This page is intentionally left blank